

# Dependence of the acoustoelastic properties and texture of an orthorhombic polycrystalline aggregate on stress

J. Lewandowski, Warsaw, Poland

Received February 27, 2004; revised January 15, 2005  
Published online: April 10, 2006 © Springer-Verlag 2006

**Summary.** The propagation of ultrasonic plane waves in a solid bulk sample is considered for the case when the sample material is of the form of a polycrystalline aggregate (e.g., steel) made of crystallites of the highest cubic symmetry. The crystallite orientation distribution is assumed to be such that it implies the orthorhombic symmetry of the macroscopic (effective) acoustoelastic properties of the polycrystalline aggregate. Moreover, the sample is assumed to be subjected to an increasing stress, the principal directions of the stress being coincident with the axes of the orthorhombic symmetry of the bulk sample. It is assumed that the ultrasonic waves also propagate and are linearly polarized in the directions coincident with the axes of the orthorhombic symmetry. The Voigt's averaging procedure and Jaynes' principle of maximum Shannon entropy are accepted as a reliable basis for the evaluation of the influence of the changes in stress on both the effective acoustoelastic properties of the polycrystalline aggregate and the probability density function of the crystallite orientation in the sample. In this way, an algorithm is prepared which enables us to evaluate numerically these effects under the assumption that the single-crystallite elastic moduli are constant. Some results obtained by using this algorithm are presented for the case of a plane increasing stress.

## 1 Introduction

Acoustoelasticity is often utilized as a tool for the nondestructive evaluation of active and residual stress within structural materials. Most of these materials are actually polycrystalline aggregates (e.g., steel). Some forming processes of a polycrystalline aggregate (e.g., rolling, drawing, forging) are accompanied by plastic deformation which always leaves the crystallites (grains) in certain preferred orientations called the texture. Hence, the anisotropic overall response of the textured polycrystalline aggregate called the effective response to an external load. The acoustoelastic technique of evaluating the texture and stress is based on the observation and theoretical predictions that the speeds at which elastic waves propagate through a textured and prestressed body depend on the propagation and polarization directions, texture as well as on the state of applied or residual stress to which the body is subjected. In this paper, such stress is called the background stress. The explanation of the dependence of the propagation properties of a polycrystalline aggregate on the background stress is based on the assumption that the strain energy is a cubic function of the strain. From this assumption the constitutive relation between stress and strain is obtained. Consequently, the acoustoelastic

response of the material is characterized by the coefficients of the quadratic and cubic terms in the strain energy, the coefficients being called the second- and third-order elastic constants (stiffness tensors), respectively. This response is obtained by considering the motion of the elastic plane wave with infinitesimal stress and displacement amplitude superposed on a state of finite homogeneous background deformation of the material. The usual result of such analysis is a set of equations for the propagation velocities of plane waves as functions of the strain, the coefficients in the equations being particular combinations of the second- and third-order elastic constants. Therefore, the procedure of estimating the acoustoelastic response of a material to an external load may start from evaluating the second- and third-order elastic constants involved in the problem under consideration. The works of G. C. Johnson [1]–[3] are examples of utilizing this concept. In [1]–[3] Johnson provides methods for the estimation of the effective elastic and acoustoelastic constants for the textured materials that exhibit transversely isotropic and orthorhombic symmetry, respectively, the methods being based on the knowledge of the elastic constants of the constituent crystals and the orientation distribution of the grains within the aggregate.

In the present work, a statistical ensemble is considered of bulk samples of the examined prestressed polycrystalline aggregate with the acoustoelastic properties exhibiting the orthorhombic symmetry. The attention is focused on a subdomain of a bulk sample, the subdomain being acted on by an ultrasonic transducer of such radiation properties that ensure the effective acoustoelastic response to be a plane and linearly polarized ultrasonic wave propagating through the sample, the directions of the propagation and polarization being coincident with the axes of the orthorhombic symmetry of the effective acoustoelastic properties of the sample. The principal directions of the background stress are also assumed to be coincident with three perpendicular to each other axes of the orthorhombic symmetry of the sample.

To analyze the acoustoelastic response, the effective modulus concept [4] is applied to a subdomain of the bulk sample. The subdomain is assumed to be enough large to enable us to measure in the subdomain the phase velocity of the ultrasonic waves and to assume that the subdomain contains a statistical ensemble of crystallites. This analysis yields relationships which allow us to compare the values of the phase velocities predicted by utilizing the effective modulus concept with that obtained from ultrasonic measurements. Similarly as in papers [5]–[7] and for the reason explained in [5, p. 238], and quoted in the paper in the fourth section, the Voigt [8] averaging procedure and Jaynes' [9] principle of maximum Shannon entropy are employed in this paper as a reliable basis for estimating the texture and the tensor of the effective elastic stiffness (or compliance) moduli of the subdomain of the polycrystalline aggregate from known (e.g., measured) values of phase velocities of ultrasonic waves propagating through the subdomain. Therefore, in the presented analysis, the texture is estimated in the maximum-entropy approximation, contrasting with Johnson's analysis [1]–[3] where the texture is treated as a known quantity. The possibility of such estimations follows from the facts that, on one hand, every component of the tensor of the effective elastic stiffness (or compliance) moduli can be expressed in terms of the effective density and phase velocities of ultrasonic waves propagating through the subdomain. On the other hand, every component of the tensor of the effective elastic moduli of a polycrystalline aggregate can be estimated by using the Voigt averaging procedure which consists in assembly averaging the elastic moduli (stiffness or compliance) of a single crystallite in the subdomain of the polycrystalline aggregate, i.e., in weighting each of the elastic moduli of the single crystallite by the probability density function of the single-crystallite orientation. This function defines the texture of the subdomain of the polycrystalline aggregate under consideration.

In the paper, as far as the probability density function of the crystallite orientation goes, it is assumed that this function is in the form implied by the Jaynes' [9] principle of maximum Shannon entropy and, therefore, fulfils both the normalization condition and all the conditions (relationships) involved in applying the Jaynes' principle. These relationships express effective material parameters (the density and elastic stiffness moduli) in terms of observables (velocities of ultrasonics). In the paper, the effective acoustoelastic properties are represented by the respective effective stiffness moduli of the polycrystalline aggregate or by the phase velocities of ultrasonic waves.

In this way, the most important concepts and methods have been mentioned briefly which enable us to gain the purpose of the paper. The purpose consists in evaluating the changes in both the acoustoelastic properties and texture of the material (steel), the changes being caused by varying (increasing) background plane stress. If the values of the applied or residual stress are sufficiently small, no plastic deformation occurs and the single-crystallite elastic moduli are constant. In the paper, the numerical evaluations are performed for the plane stress increasing from 1 MPa to 750 MPa in 750 equal steps, the material being assumed to be characterized by the same values of the density and elastic stiffness moduli as bcc Fe. The scope of the paper is confined to obtaining an algorithm for reaching the purpose of the paper, examining the properties of the algorithm by performing numerical experiments and appreciating in this way the suitability of the algorithm for giving the computer support in acoustoelastic experiments, especially in the range of ultrasonic non-destructing testing. The method is applicable for the determination of the changes in acoustoelastic properties and texture caused by both applied and residual stresses in materials of general loading histories, including plastic deformation in accordance with the discussion of Man and Lu [10]. The preliminaries of constructing the algorithm are presented in the next (second) section of the work. The algorithm for the most complex case is outlined in the third section. For this case, the influence of background stress on the changes in the acoustoelastic properties and texture of the polycrystalline material is investigated. Examples of numerical results, discussion and final remarks are presented in the fourth section for the case of a plane increasing stress. Some conclusions following from the results are given in the fifth section of the paper.

## 2 Formulation of the problem

The propagation of plane ultrasonic waves is considered in a prestressed bulk sample made of textured polycrystalline aggregates with the effective (macroscopic) acoustoelastic properties exhibiting orthorhombic symmetry, the medium being composed of cubic crystallites with the highest symmetry. In the subsequent considerations, the bulk sample is treated as belonging to a statistical ensemble of identical orthorhombic bulk samples made of the polycrystalline aggregate under consideration. Suppose an Euler orthogonal reference system  $Ox_1x_2x_3$  with the axes  $Ox_1$ ,  $Ox_2$  and  $Ox_3$  is suitably chosen for the sample; for example, in the case of a rolled plate,  $Ox_1$  could coincide with the rolling direction, the axes  $Ox_2$  and  $Ox_3$  being transverse to the rolling direction and normal to the rolling plane, respectively. Then the planes  $x_1x_2$ ,  $x_2x_3$  and  $x_3x_1$  are the planes of mirror symmetry connected with the orthorhombic symmetry of the effective acoustoelastic properties of the polycrystalline bulk sample. The unit vectors along the directions of the axes  $Ox_1$ ,  $Ox_2$  and  $Ox_3$  are denoted by  $\mathbf{e}_1$ ,  $\mathbf{e}_2$  and  $\mathbf{e}_3$ , respectively. Throughout the remainder of the paper, all equations, relations and formulae are written with locating the vector and tensor quantities as well as the orientations and coordinates to the  $Ox_1x_2x_3$  reference

system. Then the position vector  $\mathbf{x}$  can be written as  $\mathbf{x} = (x_1x_2x_3)$  where  $x_i = \mathbf{x} \cdot \mathbf{e}_i$ ,  $i = 1, 2, 3$ . The other orthogonal reference system  $0X_1X_2X_3$  is supposed to be chosen for a single cubic crystallite, the axes being chosen in the crystallographic directions [100], [010] and [001], respectively. The unit vectors along the directions of the axes  $0X_1$ ,  $0X_2$  and  $0X_3$  are denoted by  $\mathbf{E}_1$ ,  $\mathbf{E}_2$  and  $\mathbf{E}_3$ , respectively. In the subsequent considerations, the orientation of a single crystallite within the polycrystalline sample is defined by giving the values of three Eulerian angles,  $\theta$ ,  $\varphi$  and  $\phi$ , of the axes  $0X_1$ ,  $0X_2$  and  $0X_3$  relative to the sample axes,  $0x_1$ ,  $0x_2$  and  $0x_3$ . The notations  $\theta$  ( $\theta = \cos^{-1}(\mathbf{E}_3 \cdot \mathbf{e}_3) \doteq \cos^{-1} \xi$ ),  $\varphi$  and  $\phi$  stand for the angle of nutation, precession and proper rotation, respectively, where  $0 \leq \theta \leq \pi$ ,  $0 \leq \varphi \leq 2\pi$ ,  $0 \leq \phi \leq 2\pi$ .

The subsequent considerations are concerned with a statistical ensemble of identical bulk samples made of the examined prestressed polycrystalline aggregate. The samples are made of cubic crystallites with different orientations. Each of the samples is subjected to the background stress,  $\sigma^0(\mathbf{x})_{ij}$  ( $i, j = 1, 2, 3$ ). It is assumed that the principal directions of the background stress,  $\sigma^0(\mathbf{x})_{ij}$ , coincide with the symmetry axes  $0x_1$ ,  $0x_2$  and  $0x_3$ . Consider the case when the prestressed polycrystalline aggregate is acted upon by an ultrasonic transducer and denote the displacement response and equivalent stress response of the polycrystalline aggregate to this dynamic loading by  $\mathbf{u}(\mathbf{x}, t)$  and  $\sigma_{ij}(\mathbf{x}, t)$ , respectively. Suppose that the transducer oscillates with the ultrasonic angular frequency  $\omega$  in such a way that the average displacement response and equivalent average stress response,  $\langle \mathbf{u}(\mathbf{x}, t) \rangle$  and  $\langle \sigma_{ij}(\mathbf{x}, t) \rangle$ , are of the form of a displacement ultrasonic wave and equivalent stress ultrasonic wave, respectively, propagating through the polycrystalline medium. The bracket angles,  $\langle \dots \rangle$ , denote averaging over the statistical ensemble of macroscopically identical samples of the polycrystalline aggregate. In the remainder of the paper, every average value of a random variable will be taken to be an assembly average unless specified otherwise. In this paper, the scalar field of the density  $\rho(\mathbf{x})$ , the vector field of the displacement  $\mathbf{u}(\mathbf{x}, t)$ , the tensor fields of both the stress  $\sigma_{ij}(\mathbf{x}, t)$  accompanying the displacement  $\mathbf{u}(\mathbf{x}, t)$  and background stress  $\sigma^0(\mathbf{x})_{ij}$  as well as the tensor field of the elastic stiffness moduli  $C(\mathbf{x})_{ijkl}$  are regarded as stochastic variables of the position vector  $\mathbf{x}$ .

If the displacement  $\mathbf{u}(\mathbf{x}, t)$  is small enough to enable the acceleration  $d^2\mathbf{u}(\mathbf{x}, t)/dt^2$  to be replaced by  $\partial^2\mathbf{u}(\mathbf{x}, t)/\partial t^2$ , then the displacement equations governing the motion of the linear elastic polycrystalline medium with spatially variable orientation of the crystallites may be written in the form:

$$\left\{ \left[ C(\mathbf{x})_{ijkl} + \sigma^0(\mathbf{x})_{ij} \delta_{ik} \right] u(\mathbf{x}, t)_{k,l} \right\}, \quad \check{j} = \rho(\mathbf{x}) \frac{\partial^2 u(\mathbf{x}, t)_i}{\partial t^2}, \quad i, j, k, l = 1, 2, 3, \quad (1)$$

where  $\delta_{ik}$  is the Kronecker tensor. Throughout this paper the standard tensor indicial notation is used where repeated indices imply summation unless stated otherwise. It may be said that Eq. (1) differ from some equations of such papers as [11]–[13] in having a stochastic form, the randomness being taken into account under the assumption that both the elastic stiffness moduli  $C(\mathbf{x})_{ijkl}$  and the background stress  $\sigma^0(\mathbf{x}_{ij})$  vary only slightly over the distances of the wavelengths. Then the quantities  $L(\mathbf{x}) = C(\mathbf{x})_{ijkl}$ ,  $\sigma^0(\mathbf{x})_{ij}$ ,  $\mathbf{u}(\mathbf{x}, t)$ ,  $\rho(\mathbf{x})$  can be split into their means  $\langle L(\mathbf{x}) \rangle$  and the corresponding fluctuations  $\delta L(\mathbf{x})$ :

$$\begin{aligned} C(\mathbf{x})_{ijkl} &= \langle C(\mathbf{x})_{ijkl} \rangle + \delta C(\mathbf{x})_{ijkl}, \quad \mathbf{u}(\mathbf{x}, t) = \langle \mathbf{u}(\mathbf{x}, t) \rangle + \delta \mathbf{u}(\mathbf{x}, t), \\ \sigma^0(\mathbf{x})_{ij} &= \langle \sigma^0(\mathbf{x})_{ij} \rangle + \delta \sigma^0(\mathbf{x})_{ij}, \quad \rho(\mathbf{x}) = \langle \rho(\mathbf{x}) \rangle + \delta \rho(\mathbf{x}). \end{aligned} \quad (2)$$

On substituting Eq. (2) into Eq. (1) and averaging we arrive at the following equations for  $\langle \mathbf{u}(\mathbf{x}, t) \rangle$ , after employing  $\langle \delta L(\mathbf{x}) \rangle = 0$  and assuming that the fluctuations  $\delta L(\mathbf{x})$  are so small

that  $[\langle \delta C(\mathbf{x})_{ijkl} \delta u(\mathbf{x}, t)_{k,l} \rangle]_j$ ,  $[\langle \delta \sigma^0(\mathbf{x})_{ij} \delta u(\mathbf{x}, t)_{k,j} \rangle]_j$ ,  $\langle \delta \rho(\mathbf{x}) \{ \partial^2 \delta u(\mathbf{x}, t)_i / \partial t^2 \} \rangle$  can be omitted in the analysis:

$$\left\{ \left[ \langle C(\mathbf{x})_{ijkl} \langle u(\mathbf{x}, t)_{k,l} \rangle \right]_j + \langle \sigma^0(\mathbf{x})_{ij} \langle u(\mathbf{x}, t)_{k,jl} \rangle \delta_{ik} \right\} - \langle \rho(\mathbf{x}) \rangle \frac{\partial^2 \langle u(\mathbf{x}, t)_i \rangle}{\partial t^2} = 0, \quad i, j, k, l = 1, 2, 3. \quad (3)$$

Now the effective modulus concept [4] seems to be very useful for employing Eq. (3) to our purpose. This hypothesis implies that for the considered polycrystalline aggregate it is possible to find such a fictitious homogeneous equivalent material (monocrystal) that the behavior of the equivalent monocrystal in different circumstances is the same as the assembly averaged behavior of the polycrystalline aggregate under the same conditions. Then the material parameters, which characterize the equivalent monocrystal, for example, the density  $\rho(\mathbf{x})^{eff}$ , and the tensor of the elastic stiffness moduli,  $C(\mathbf{x})_{ijkl}^{eff}$ , are called the effective density and the tensor of the effective elastic stiffness moduli, respectively, of the polycrystalline aggregate under consideration, the tensor of the effective elastic stiffness moduli,  $C(\mathbf{x})_{ijkl}^{eff}$ , exhibiting the orthorhombic symmetry. In the case considered in this paper, the overall (assembly averaged) response,  $\langle \mathbf{u}(\mathbf{x}, t) \rangle$  to the load of the ultrasonic transducer is assumed to be of the form of plane ultrasonic waves. Therefore, the orthorhombic symmetry of the tensor of effective elastic stiffness,  $C(\mathbf{x})_{ijkl}^{eff}$ , of the considered polycrystalline aggregate is revealed by the overall response of the prestressed polycrystalline aggregate to the load of the ultrasonic transducer, i.e., by the symmetry of the macroscopic propagation parameters of the effective ultrasonic waves,  $\langle \mathbf{u}(\mathbf{x}, t) \rangle$  the propagation of the effective ultrasonic waves in the prestressed material being governed by equations of motion (3).

Moreover, Eq. (3) imply the following equations for the effective material parameters of the prestressed polycrystalline aggregate:

$$\rho(\mathbf{x})^{eff} = \langle \rho(\mathbf{x}) \rangle, \quad C(\mathbf{x})_{ijkl}^{eff} = \langle C(\mathbf{x})_{ijkl} \rangle, \quad i, j, k, l = 1, 2, 3. \quad (4)$$

$\rho(\mathbf{x})^{eff}$  denotes the effective density which is assumed in this paper to be equal to the density of the polycrystalline aggregate averaged over the volume of a single bulk sample of the material. It means that  $\langle \rho(\mathbf{x}) \rangle$  in Eq. (3) denotes the density averaged over the sample volume and may be regarded as a material parameter,  $\rho^{eff} = \langle \rho(\mathbf{x}) \rangle$ , of the polycrystalline aggregate,  $\rho^{eff}$  being constant and independent of the position vector  $\mathbf{x}$  in the polycrystalline aggregate. Let  $\rho_{cr}$  denote the density of a single cubic crystallite in the polycrystalline aggregate. In numerous polycrystalline aggregates such as steel, which are used as very important materials in industry, civil engineering and so on, there are present imperfections (structure defects) such as pores, voids made by imperfect adhesion of neighbouring grains (crystallites), and impurities. Such imperfections may result in  $\rho^{eff} \neq \rho_{cr}$ . In the paper, it is assumed that the contributions of the distributions of the structure defects to the acoustoelastic anisotropy are negligibly small as compared with that of texture and stress. The problem is also formulated under the assumption that the single-crystallite elastic moduli  $c_{11}$ ,  $c_{12}$  and  $c_{44}$  retain their constant values. The effective material parameters are involved in both the equations of motion governing the propagation of the considered waves through the subdomain of the polycrystalline aggregate and in the relationships between the phase velocities of these waves and the effective material parameters of the medium,

In general, due to the different orientations of the grains, which vary from crystallite to crystallite, the local physical tensor properties even of a one-component material solid, if they are referred to the Euler reference system  $0x_1x_2x_3$ , also vary from crystallite to crystallite and for this reason should be considered as functions of the position vector  $\mathbf{x} = (x_1, x_2, x_3)$ . The

different orientations of the grains also cause scattering of acoustic waves propagating through the medium and in this way result in appearing attenuation in the phenomenological description of the waves propagation even if the crystallites are perfectly elastic. Consequently, the effective elastic moduli,  $C(\mathbf{x})_{ijkl}^{eff}$ , which are involved in the equations governing the propagation of acoustic waves in such a polycrystalline medium, are in general complex if the crystallites are both perfectly and non-perfectly elastic, e.g. linearly viscoelastic. However, the values of the imaginary parts,  $\left\{C(\mathbf{x})_{ijkl}^{eff}\right\}^{(b)}$ , of all effective elastic moduli  $C(\mathbf{x})_{ijkl}^{eff}$  tend to zero with increasing length of the acoustic waves. In this paper, we are interested only in the limiting case when the absolute value of the imaginary part of each effective elastic modulus,  $\left|\left\{C(\mathbf{x})_{ijkl}^{eff}\right\}^{(b)}\right|$ , is negligibly small as compared with the corresponding real one,  $\left|\left\{C(\mathbf{x})_{ijkl}^{eff}\right\}^{(a)}\right|$ , i.e. we are interested in the limiting case  $\left|\left\{C(\mathbf{x})_{ijkl}^{eff}\right\}^{(b)}\right|/\left|\left\{C(\mathbf{x})_{ijkl}^{eff}\right\}^{(a)}\right| \ll 1$ .

As was mentioned above, both the local elastic stiffness moduli,  $C(\mathbf{x})_{ijkl}$ , of the material and the orientations of the grains (crystallites) in a sample of the polycrystalline aggregate are referred to the Euler reference system  $0x_1x_2x_3$ , the statistics of the grain orientations being described by the probability density function of the single-crystallite orientation called the texture. Therefore, in the general case the local stiffness moduli,  $C(\mathbf{x})_{ijkl}$ , even of a one-component material, vary from crystallite to crystallite and for this reason are considered as random functions of the position vector  $\mathbf{x} = (x_1, x_2, x_3)$ . On the other hand, in Eq. (4), the texture is involved in the assembly averaging (i.e., in weighting by the probability density function of the single-crystallite orientation) of elastic stiffness moduli  $C(\mathbf{x})_{ijkl}$ . This averaging enables us to evaluate  $C(\mathbf{x})_{ijkl}^{eff}$ . Therefore, the effective stiffness moduli do not depend on the position vector  $\mathbf{x}$  (i.e.  $C(\mathbf{x})_{ijkl}^{eff} = C_{ijkl}^{eff}$ ) if the probability density function of the single-crystallite orientation is also independent of  $\mathbf{x}$ .

Fortunately, ultrasonic experiments reveal that in calculating  $C(\mathbf{x})_{ijkl}^{eff}$  for numerous acoustic applications and purposes, which are of great practical significance, we are dealing with such subdomains in which it is both possible to determine in a good approximation and allowed to employ weight functions (textures) independent of  $\mathbf{x}$ . Therefore, the concept of the texture independence of  $\mathbf{x}$  consists in describing the texture in a finite subdomain of the sample by making use of the probability density function of the crystallite orientation,  $p(\theta, \varphi, \phi)$ , the function  $p(\theta, \varphi, \phi)$  being independent of the position vector  $\mathbf{x}$ . Then  $p(\theta, \varphi, \phi)d\theta d\varphi d\phi$  expresses the probability that a crystallite in the subdomain of the sample has an orientation described by the Euler angles  $\theta$ ,  $\varphi$  and  $\phi$ , lying in the intervals  $\langle \theta, \theta + d\theta \rangle$ ,  $\langle \varphi, \varphi + d\varphi \rangle$  and  $\langle \phi, \phi + d\phi \rangle$ , respectively.

The assumption that the texture  $p(\theta, \varphi, \phi)$  is independent of the position vector  $\mathbf{x}$  concerns the use of three measuring scales, the smallest of which refers to a microelement (single crystal) of the bulk sample of the polycrystalline aggregate. Next an intermediary scale is introduced referred to as mesodomain that contains a statistical ensemble of microelements. This mesodomain is interpreted to be much smaller than the macroscopic domain (the largest scale) of the entire material body (bulk sample), but is much larger than the domain of a microelement. At this moment we also touch upon the technique and the size of the equipments employed in ultrasonic measuring in the polycrystalline aggregates. Briefly speaking, it is reasonable to ask about the *smallest size* of a mesodomain at which performing the ultrasonic measurements with employing the selected technique and equipments is still possible. In this context, such terms as the *local* texture and *local* properties of the sample material revealed by or deduced from ultrasonic measurements do not mean the texture

and properties in a point  $\mathbf{x}$  in the sample under study but mean the texture and properties at every point of the sample material filling a mesodomain centered at the point  $\mathbf{x}$  and having at least the *smallest size* at which performing the ultrasasonic measurements is still possible. In this sense we treat the texture  $p(\theta, \varphi, \phi)$  and effective elastic stiffness moduli  $C_{ijkl}^{eff}$  as quantities independent of  $\mathbf{x}$  within the mesodomain of the *smallest size*, corresponding to the intermediary scale and being defined by the conditions of performing the ultrasasonic measurements. It should perhaps be emphasized that in numerous practically important cases the sizes of the subdomains of polycrystalline materials, in which  $p(\theta, \varphi, \phi)$  and  $C_{ijkl}^{eff}$  may be regarded (at least in a good approximation) as independent of  $\mathbf{x}$ , are relatively large or even very large as compared with the subdomain of the smallest size. In such cases, supposing  $p(\theta, \varphi, \phi)$  and elastic stiffness moduli  $C_{ijkl}$  to be independent of  $\mathbf{x}$  does not require employing the concept of the mesodomain of the *smallest size*.

If the principal directions of the plane background stress,  $\sigma^0(\mathbf{x})_{ij}$ , coincide with the axes  $0x_1$ ,  $0x_2$  and  $0x_3$  of the orthorhombic symmetry, then the stress  $\sigma^0(\mathbf{x})_{ij}$ , does not induce any change in the symmetry of the effective acoustoelastic properties of the bulk sample under consideration but induces changes in the values of the respective indices of the acoustoelastic anisotropy which corresponds to the orthorhombic symmetry of the sample. Therefore, the effective dynamic properties of the prestressed polycrystalline aggregate under study, which exhibit orthorhombic symmetry, and its single cubic crystallite (monocrystalline grain) are defined by the effective elastic stiffness moduli  $\{C_{11}^{eff}, C_{22}^{eff}, C_{33}^{eff}, C_{44}^{eff}, C_{55}^{eff}, C_{66}^{eff}, C_{12}^{eff}, C_{13}^{eff}, C_{23}^{eff}\}$  and the single-crystal elastic moduli  $\{c_{11}, c_{12}, c_{44}\}$ , respectively.

In the paper, for the sake of brevity and convenience, the following normalized tensor quantities are used:

$$\tilde{c}_{ij} = c_{ij}/\rho^{eff}, \quad \tilde{C}_{ij} = C_{ij}^{eff}/\rho^{eff}, \quad \tilde{\sigma}_{ij}^0 = \sigma_{ij}^0/\rho^{eff} \quad i, j = 1, 2, 3. \quad (5)$$

Now we assume that it is justified to regard the texture,  $p(\xi, \varphi, \theta)$ , and, consequently, the effective elastic stiffness moduli,  $C_{ijkl}^{eff}$ , as quantities independent of  $\mathbf{x}$  in the sense explained above, i.e., in a subdomain  $\Omega_s$  centered at  $\mathbf{x}_s$ . Then we arrive at the following equations for  $C(\mathbf{x})_{ijkl}^{eff} = C_{ijkl}^{eff}$  where  $\mathbf{x} \in \Omega_s$ , after employing the Voigt [8] averaging procedure as a suitable one for evaluating  $C_{ijkl}^{eff} = \langle C(\mathbf{x})_{ijkl} \rangle = \langle C(\mathbf{x}_s)_{ijkl} \rangle$ :

$$C_{ijkl}^{eff} = \langle C(\mathbf{x}_s)_{ijkl} \rangle, \quad \langle C(\mathbf{x}_s)_{ijkl} \rangle = \int_{-1}^1 d\xi \int_0^{2\pi} d\varphi \int_0^{2\pi} d\phi C(\mathbf{x}_s)_{ijkl} P(\xi, \varphi, \phi), \quad (6)$$

$C(\mathbf{x}_s)_{ijkl} = t(\xi, \varphi, \phi)_{mi} t(\xi, \varphi, \phi)_{nj} t(\xi, \varphi, \phi)_{pk} t(\xi, \varphi, \phi)_{ql} c_{mnpq}$ ,  $i, j, k, l, m, n, p, q = 1, 2, 3$ .  $c_{mnpq}$ ,  $m, n, p, q = 1, 2, 3$ , denote the elastic stiffness moduli of a single crystallite (for example,  $c_{11}$ ,  $c_{12}$  and  $c_{44}$  in the case of cubic crystallite), and  $t(\xi, \varphi, \phi)_{im}$  stands for the components of the transformation matrix  $\mathbf{t}(\xi, \varphi, \phi)$  relating  $x_i$  to  $X_i$  in the following way:

$$X_i = t(\xi, \varphi, \phi)_{ij} x_j \quad \text{where } \xi \doteq \cos \theta. \quad (7)$$

Therefore, the displacement equations of motion governing the wave propagation through a subdomain  $\Omega_s$  of a bulk sample, in which  $p(\xi, \varphi, \phi)$  and  $C_{ijkl}^{eff} = \langle C(\mathbf{x}_s)_{ijkl} \rangle$  may be regarded as being independent of  $\mathbf{x}$ , can be deduced immediately from Eq. (3) as having the following form:

$$(\tilde{C}_{ijkl} + \tilde{\sigma}_{jl}^0 \delta_{ik}) \frac{\partial^2 \langle u(\mathbf{x}, t)_k \rangle}{\partial x_j \partial x_i} = \frac{\partial^2 \langle u(\mathbf{x}, t)_i \rangle}{\partial t^2}, \quad i, j, k, l = 1, 2, 3. \quad (8)$$

Let us remind that in numerical analysis of the the present work we consider the case when the prestressed polycrystalline aggregate is acted on by the ultrasasonic transducer which oscillates

with the ultrasonic angular frequency  $\omega$  in such a way that the effective response of the polycrystalline aggregate to this dynamic loading is of the form of a displacement ultrasonic wave,  $\langle \mathbf{u}(\mathbf{x}, t) \rangle$ , which propagates through the polycrystalline medium, the motion of the medium being governed by Eq. (8). Moreover, we seek simple particular solutions,  $\langle \mathbf{u}(\mathbf{x}, t) \rangle$ , to Eq. (8) in the form of plane and linearly polarized ultrasonic waves, each of the directions of the propagation  $\mathbf{n}$  ( $|\mathbf{n}| = 1$ ) and polarization  $\mathbf{p}$  ( $|\mathbf{p}| = 1$ ) being coincident with one of the axes  $0x_1$ ,  $0x_2$  and  $0x_3$  of the reference system  $0x_1x_2x_3$ . It means that the directions of the propagation and polarization are also coincident with the axes of the orthorhombic symmetry and with the principal axes of the background stress. Then the particular solutions to Eq. (8) (ultrasonic plane and linearly polarized waves) being of interest for us may be written as follows:

$$\langle \mathbf{u}(\mathbf{x}, t) \rangle = \mathbf{p} u_0 \exp[ik_{np}(\mathbf{n} \cdot \mathbf{x} - V_{np}t)] = \mathbf{p} u_0 \exp([ik_{np}(\mathbf{n} \cdot \mathbf{x} - \omega t)]. \quad (9)$$

$V_{np}$  denotes the phase velocity of a wave propagating in the direction of the unit vector  $\mathbf{n} = (n_1, n_2, n_3)$  and being polarized in the direction of the unit vector  $\mathbf{p} = (p_1, p_2, p_3)$ , where  $n_i = \mathbf{n} \cdot \mathbf{e}_i$  and  $p_i = \mathbf{p} \cdot \mathbf{e}_i$ ,  $i = 1, 2, 3$ ,  $u_0$  stands for the amplitude of the displacement wave, and  $k_{np}$  stands for the wave number,  $k_{np} = \omega/V_{np}$ .

In every heterogeneous elastic body, the ultrasonic velocities  $V_{np}$  depend on the effective density  $\rho^{eff}$  and the tensor of the so-called effective dynamic moduli  $C_{ijkl}^{eff}$  of the elastic stiffness as well as on the frequency  $\omega$ . In the limit, as the ultrasonic wavelength increases to infinity (or the frequency diminishes to zero), the dynamic effective moduli in these relations may be replaced by the static effective moduli. Such an approximation, which was used in numerous papers, will also be employed from now on in this paper (Eq. (6)) where the effective moduli  $C_{ijkl}^{eff}$  will be taken to be the static effective ones.

On substituting the plane wave solution (9) into Eq. (8), one obtains the so-called Kelvin equations for the displacement amplitude  $\mathbf{U} = u_0 \mathbf{p}$ ,

$$\left[ \tilde{C}_{ijkl} n_j n_l + (\tilde{\sigma}_{ji}^0 n_j n_l - V_{np}^2) \delta_{ik} \right] p_k = 0, \quad i, j, k, l = 1, 2, 3. \quad (10)$$

Equations (8) and (10) correspond to some results of Refs. [12] and [13].

Now let us insert successively into Eq. (8) nine forms of the supposed partial solution (9) corresponding to nine wave modes propagating in the direction of the unit vector  $\mathbf{n} = (n_1, n_2, n_3)$  and being polarized in the direction of the unit vector  $\mathbf{p} = (p_1, p_2, p_3)$ , the vectors  $\mathbf{n}$  and  $\mathbf{p}$  being independently of each other of the forms

$$\mathbf{n}, \mathbf{p} = (1, 0, 0), (0, 1, 0), (0, 0, 1). \quad (11)$$

In this way we can deduce that the satisfaction of Eq. (8) by each of the nine modes (11) successively requires the following relationships to be fulfilled:

$$\begin{aligned} \tilde{C}_{11} &= V_{11}^2 - \tilde{\sigma}_{11}^0, & \tilde{C}_{22} &= V_{22}^2 - \tilde{\sigma}_{22}^0, & \tilde{C}_{33} &= V_{33}^2 - \tilde{\sigma}_{33}^0, & \tilde{C}_{44} &= V_{23}^2 - \tilde{\sigma}_{22}^0 = V_{32}^2 - \tilde{\sigma}_{33}^0, \\ \tilde{C}_{55} &= V_{13}^2 - \tilde{\sigma}_{11}^0 = V_{31}^2 - \tilde{\sigma}_{33}^0, & \tilde{C}_{66} &= V_{12}^2 - \tilde{\sigma}_{11}^0 = V_{21}^2 - \tilde{\sigma}_{22}^0. \end{aligned} \quad (12)$$

In accordance with the abbreviation defined below Eqs. (9),  $V_{ij}$  ( $i, j = 1, 2, 3$ ), denotes the phase velocity of a plane wave (9) propagating through the sample in the direction of the axis  $0x_i$  of the reference system  $0x_1x_2x_3$ , the wave being polarized in the direction of the axis  $0x_j$ . It should perhaps be stressed that in the relationships (12) there are involved the components in the principal directions,  $\tilde{\sigma}_{11}^0$ ,  $\tilde{\sigma}_{11}^0$  and  $\tilde{\sigma}_{33}^0$ , of the background stress  $\tilde{\sigma}_{ij}^0$ . For this reason, in the remainder of the paper  $\tilde{\sigma}_{11}^0$ ,  $\tilde{\sigma}_{22}^0$  and  $\tilde{\sigma}_{33}^0$  are the only components of the background  $\tilde{\sigma}_{ij}^0$  interesting for us.

Moreover, the satisfaction of Eq. (8) requires that

$$\begin{aligned} \tilde{C}_{61} = \tilde{C}_{51} = \tilde{C}_{26} = \tilde{C}_{46} = \tilde{C}_{45} = \tilde{C}_{35} = \tilde{C}_{16} = \tilde{C}_{56} = \tilde{C}_{62} = \tilde{C}_{42} \\ = \tilde{C}_{54} = \tilde{C}_{34} = \tilde{C}_{15} = \tilde{C}_{65} = \tilde{C}_{64} = \tilde{C}_{24} = \tilde{C}_{53} = \tilde{C}_{43} = 0. \end{aligned} \quad (13)$$

Equations (13) are the orthorhombic symmetry requirements for the tensor components  $\tilde{C}_{ijkl}$  appearing in these equations (conditions).

It can easily be seen that Eq. (12) give the facilities for doing some useful evaluations for prestressed polycrystalline aggregates with orthorhombic macroscopic symmetry. The utility of Eq. (12) can be illustrated by the two following examples:

- (i) If the values of the nine quantities  $V_{11}, V_{22}, V_{33}, V_{12}, V_{21}, V_{13}, V_{23}, V_{31}$  and  $V_{32}$  are known (from measurements or theoretical predictions) then the background stress components in three principal directions,  $\sigma_{11}^0, \sigma_{22}^0, \sigma_{33}^0$ , as well as the effective material parameters  $\tilde{C}_{11}, \tilde{C}_{22}, \tilde{C}_{33}, \tilde{C}_{44}, \tilde{C}_{55}$  and  $\tilde{C}_{66}$ , can be evaluated immediately from Eq. (12).
- (ii) In another situation, in addition to  $\tilde{\sigma}_{11}^0, \tilde{\sigma}_{22}^0, \tilde{\sigma}_{33}^0, \tilde{C}_{11}, \tilde{C}_{22}, \tilde{C}_{33}, \tilde{C}_{44}, \tilde{C}_{55}$  and  $\tilde{C}_{66}$ , it is also possible to evaluate the probability density function of the crystallite orientation,  $p(\theta, \varphi, \varphi)$ . An example of such a simplified situation is as follows:

If  $\tilde{\sigma}_{11}^0 \neq 0, \tilde{\sigma}_{22}^0 \neq 0$  and  $\tilde{\sigma}_{33}^0 = 0$  (the case of plane background stress), and if the values of the twelve quantities  $V_{11}, V_{22}, V_{33}, V_{12}, V_{21}, V_{13}, V_{23}, V_{31}, V_{32}, \tilde{c}_{11}, \tilde{c}_{12}$  and  $\tilde{c}_{44}$  are known at the start of computing, then the probability density function of the crystallite orientation,  $p(\theta, \varphi, \varphi)$ , can be estimated by making use of Eqs. (6), (12), the normalization condition for  $p(\theta, \varphi, \varphi)$  as well as by utilizing the Jaynes' [9] principle of the maximum Shannon entropy as a constructive criterion for setting up the function  $p(\theta, \varphi, \varphi)$  on the basis of partial knowledge given by Eq. (12). In the case of  $\tilde{\sigma}_{11}^0 = \tilde{\sigma}_{22}^0 = \tilde{\sigma}_{33}^0 = 0$  or  $\tilde{\sigma}_{11}^0 \approx 0, \tilde{\sigma}_{22}^0 \approx 0, \tilde{\sigma}_{33}^0 \approx 0$  it is sufficient to know, as it follows from Eqs. (12) and [14, Eqs. (22)], the values of only six quantities: three velocities (e.g.,  $V_{11}, V_{13}, V_{33}$ ) and  $\tilde{c}_{11}, \tilde{c}_{12}$  and  $\tilde{c}_{44}$ . In the two last cases it is also possible to evaluate the changes in  $V_{11}, V_{22}, V_{33}, V_{12}, V_{21}, V_{13}, V_{23}, V_{31}, V_{32}, \tilde{C}_{11}, \tilde{C}_{22}, \tilde{C}_{33}, \tilde{C}_{44}, \tilde{C}_{55}, \tilde{C}_{66}$  and  $p(\theta, \varphi, \varphi)$  with increasing  $\tilde{\sigma}_{11}^0, \tilde{\sigma}_{22}^0$  and  $\tilde{\sigma}_{33}^0$  by small known steps  $\Delta\tilde{\sigma}_{11}^0, \Delta\tilde{\sigma}_{22}^0$  and  $\Delta\tilde{\sigma}_{33}^0$ . The proposal of an algorithm for such evaluations will be presented in the next Section.

### 3 Algorithm

In this paper, Eqs. (6), (12) and the Jaynes' [9] principle of the maximum Shannon entropy are the basis for making up an algorithm enabling us to estimate the previously mentioned changes in the orthorhombic acoustic anisotropy and texture of prestressed ( $\tilde{\sigma}_{11}^0 \neq 0, \tilde{\sigma}_{22}^0 \neq 0, \tilde{\sigma}_{33}^0 \neq 0$ ) polycrystalline aggregates, the changes being caused by increasing background stress  $\tilde{\sigma}_{ij}^0$ . Now let us present the preliminaries of this algorithm.

When Eqs. (12) are considered together with Eq. (6) and [14, Eq. (4)], we obtain for the case of  $\tilde{\sigma}_{11}^0 \neq 0, \tilde{\sigma}_{22}^0 \neq 0, \tilde{\sigma}_{33}^0 \neq 0$

$$\tilde{C}_{11} = \tilde{c}_{11} - 2(\tilde{c}_{11} - \tilde{c}_{12} - 2\tilde{c}_{44})\langle r_1(\xi, \varphi, \phi) \rangle = V_{11}^2 - \tilde{\sigma}_{11}^0, \quad (14)$$

$$\tilde{C}_{22} = \tilde{c}_{11} - 2(\tilde{c}_{11} - \tilde{c}_{12} - 2\tilde{c}_{44})\langle r_2(\xi, \varphi, \phi) \rangle = V_{22}^2 - \tilde{\sigma}_{22}^0, \quad (15)$$

$$\tilde{C}_{33} = \tilde{c}_{11} - 2(\tilde{c}_{11} - \tilde{c}_{12} - 2\tilde{c}_{44})\langle r_3(\xi, \varphi, \phi) \rangle = V_{33}^2 - \tilde{\sigma}_{33}^0, \quad (16)$$

$$\tilde{C}_{44} = \tilde{c}_{44} + (\tilde{c}_{11} - \tilde{c}_{12} - 2\tilde{c}_{44})\langle r_4(\xi, \varphi, \phi) \rangle = V_{23}^2 - \tilde{\sigma}_{22}^0, \quad (17)$$

$$\tilde{C}_{55} = \tilde{c}_{44} + (\tilde{c}_{11} - \tilde{c}_{12} - 2\tilde{c}_{44})\langle r_5(\xi, \varphi, \phi) \rangle = V_{13}^2 - \tilde{\sigma}_{11}^0, \quad (18)$$

$$\tilde{C}_{66} = \tilde{c}_{44} + (\tilde{c}_{11} - \tilde{c}_{12} - 2\tilde{c}_{44})\langle r_6(\xi, \varphi, \phi) \rangle = V_{12}^2 - \tilde{\sigma}_{11}^0, \quad (19)$$

$$\tilde{\sigma}_{11}^0 - \tilde{\sigma}_{33}^0 = V_{13}^2 - V_{31}^2, \quad \tilde{\sigma}_{22}^0 - \tilde{\sigma}_{33}^0 = V_{23}^2 - V_{32}^2, \quad \tilde{\sigma}_{11}^0 - \tilde{\sigma}_{22}^0 = V_{12}^2 - V_{21}^2, \quad (20)$$

$$\langle r_4(\xi, \varphi, \phi) \rangle = \langle r_3(\xi, \varphi, \phi) \rangle + \langle r_2(\xi, \varphi, \phi) \rangle - \langle r_1(\xi, \varphi, \phi) \rangle, \quad (21)$$

$$\langle r_5(\xi, \varphi, \phi) \rangle = 2\langle r_1(\xi, \varphi, \phi) \rangle - \langle r_2(\xi, \varphi, \phi) \rangle + \langle r_4(\xi, \varphi, \phi) \rangle, \quad (22)$$

$$\langle r_6(\xi, \varphi, \phi) \rangle = 2\langle r_1(\xi, \varphi, \phi) \rangle - \langle r_5(\xi, \varphi, \phi) \rangle, \quad (23)$$

where Eqs. (21)–(23) follow from the following definitions of  $r_1, r_2, \dots, r_6$  and some trigonometrical identities:

$$r_1 = l_1^2 l_2^2 + l_1^2 l_3^2 + l_2^2 l_3^2, \quad r_2 = m_1^2 m_2^2 + m_1^2 m_3^2 + m_2^2 m_3^2, \quad (24)$$

$$r_3 = n_1^2 n_2^2 + n_1^2 n_3^2 + n_2^2 n_3^2, \quad r_4 = m_1^2 n_1^2 + m_2^2 n_2^2 + m_3^2 n_3^2, \quad (25)$$

$$r_5 = n_1^2 l_1^2 + n_2^2 l_2^2 + n_3^2 l_3^2, \quad r_6 = l_1^2 m_1^2 + l_2^2 m_2^2 + l_3^2 m_3^2, \quad (26)$$

$$l_i = \mathbf{E}_i \cdot \mathbf{e}_1, \quad m_i = \mathbf{E}_i \cdot \mathbf{e}_2, \quad n_i = \mathbf{E}_i \cdot \mathbf{e}_3, \quad i = 1, 2, 3. \quad (27)$$

The abbreviations  $\langle r_t(\xi, \varphi, \phi) \rangle$ ,  $t = 1, 2, \dots, 6$ , in Eqs. (14)–(19) denote averaging the function  $r_t(\xi, \varphi, \phi)$  over all the crystallites in the sample, i.e.,  $\langle r_t(\xi, \varphi, \phi) \rangle$  denotes  $r_t(\xi, \varphi, \phi)$  weighted by  $p(\xi, \varphi, \phi)$ :

$$\langle r_t(\xi, \varphi, \phi) \rangle = \int_{-1}^1 d\xi \int_0^{2\pi} d\varphi \int_0^{2\pi} d\phi r_t(\xi, \varphi, \phi) p(\xi, \varphi, \phi). \quad (28)$$

Every of Eqs. (14)–(19) consists actually of two equations. In each of these equations we will distinguish its left- and right-hand part. For example, the equations  $\tilde{C}_{11} = \tilde{c}_{11} - 2(\tilde{c}_{11} - \tilde{c}_{12} - 2\tilde{c}_{44})\langle r_1(\xi, \varphi, \phi) \rangle$  and  $\tilde{c}_{11} - 2(\tilde{c}_{11} - \tilde{c}_{12} - 2\tilde{c}_{44})\langle r_1(\xi, \varphi, \phi) \rangle = V_{11}^2 - \tilde{\sigma}_{11}^0$  are the left- and right-hand part of Eqs. (14), respectively.

Let us note that the texture  $p(\xi, \varphi, \phi)$  and one of the velocities  $V_{ij}$ ,  $i, j = 1, 2, 3$ , appear in each of Eqs. (14)–(19). Hence the idea [5] of regarding equations similar to Eqs. (14)–(19) as a basis for estimating the function  $p(\xi, \varphi, \phi)$  from ultrasonic measurements of  $V_{ij}$  and by maximizing conditionally the Shannon entropy of the function  $p(\xi, \varphi, \phi)$ . From Eqs. (24)–(27), it follows that among the six expectation values  $\langle r_t(\xi, \varphi, \phi) \rangle$ ,  $t = 1, 2, \dots, 6$ , only three are linearly independent of each other. Therefore, in this paper no more than three expectation values  $\langle r_t(\xi, \varphi, \phi) \rangle$  may be involved in each considered problem of estimating the function  $p(\xi, \varphi, \phi)$  for prestressed polycrystalline aggregates with orthorhombic symmetry,  $p(\xi, \varphi, \phi)$  being estimated from the velocities  $V_{ij}$  and by using the Lagrangian multipliers method for conditional maximum of missing information (Shannon entropy).

Since the present work involves the maximum number, three, of the expectation values  $\langle r_t(\xi, \varphi, \phi) \rangle$ ,  $t = 1, 2, \dots, 6$ , which may be involved in the problem of determining the function  $p(\xi, \varphi, \phi)$  by maximizing conditionally the Shannon entropy, we choose the normalization condition

$$\langle 1 \rangle = \int_{-1}^1 d\xi \int_0^{2\pi} d\varphi \int_0^{2\pi} d\phi p(\xi, \varphi, \phi) = 1 \quad (29)$$

as well as the right-hand parts of Eqs. (14), (16) and (18) as a reliable basis for the formulation of the variational problem of the estimation of the texture  $p(\xi, \varphi, \phi)$ . The right-hand parts of Eqs. (14), (16) and (18) may be rewritten in the following forms:

$$\langle r_1(\xi, \varphi, \phi) \rangle = \frac{\bar{\sigma}_{11}^0 + \bar{c}_{11} - V_{11}^2}{2(\bar{c}_{11} - \bar{c}_{12} - 2\bar{c}_{44})}, \quad (30)$$

$$\langle r_3(\xi, \varphi, \phi) \rangle = \frac{\bar{c}_{11} - V_{33}^2}{2(\bar{c}_{11} - \bar{c}_{12} - 2\bar{c}_{44})}, \quad (31)$$

$$r_5(\xi, \varphi, \phi) = \frac{V_{13}^2 - \bar{\sigma}_{11}^0 + \bar{c}_{44}}{(\bar{c}_{11} - \bar{c}_{12} - 2\bar{c}_{44})}. \quad (32)$$

Equations (29)–(32) express the constraints which should be subject to the Shannon entropy  $I$ ,

$$I\alpha - \int_{-1}^1 d\xi \int_0^{2\pi} d\varphi \int_0^{2\pi} d\phi p(\xi, \varphi, \phi) \ln p(\xi, \varphi, \phi) \quad (33)$$

upon maximization, when the procedure of the maximum-entropy estimate [6, Appendix] is utilized for determining the function  $p(\xi, \varphi, \phi)$ . In this way we obtain the function  $p(\xi, \varphi, \phi)$  in the form

$$p(\xi, \varphi, \phi) = \frac{1}{Z} \exp[-L_1 r_1(\xi, \varphi, \phi) - L_3 r_3(\xi, \varphi, \phi) - L_5 r_5(\xi, \varphi, \phi)], \quad (34)$$

where  $1 - \ln Z$ ,  $L_1$ ,  $L_3$ , and  $L_5$  denote the Lagrangian multipliers corresponding to the conditions (29)–(32), respectively. On finding the Lagrangian multipliers  $L_1$ ,  $L_3$ ,  $L_5$  and the partition function  $Z$ , the maximum-entropy probability density function,  $p(\xi, \varphi, \phi)$  can be estimated.

The considerations of the second and current section have brought us to Eqs. (14)–(23), (29)–(32), (34), Eqs. (30)–(32) being another form of the right-hand parts of Eqs. (14)–(16), (18). In the paper, these equations are regarded as a basis for the evaluation of the changes both in the values of the ultrasonic velocities  $V_{11}$ ,  $V_{22}$ ,  $V_{33}$ ,  $V_{12}$ ,  $V_{21}$ ,  $V_{13}$ ,  $V_{23}$ ,  $V_{31}$ ,  $V_{32}$  and the values of  $L_k$ ,  $k = 1, 3, 5$ , and  $Z$ , the changes being caused by the changes in the values of the plane background stresses  $\sigma_{11}^0$ ,  $\sigma_{22}^0$ ,  $\sigma_{33}^0$ . The above mentioned quantities are connected with each other by Eqs. (14)–(23), (29), (34) in a complicated nonlinear and even functional manner. “There are no good, general methods for solving systems of more than one nonlinear equation. Furthermore, it is not hard to see why (very likely) there *never will be* any good, general methods” [15, p. 372]. For this reason, we have performed the computations for the case of plane background stress ( $\sigma_{11}^0 \neq 0$ ,  $\sigma_{22}^0 \neq 0$  and  $\sigma_{33}^0 = 0$ ) with using our own method. The computations have been performed for the background plane stress  $\sigma_{ij}^0$  with the values of  $\sigma_{11}^0$  varying in the interval [1 MPa, 750 MPa] and  $\sigma_{22}^0 = \gamma \cdot \sigma_{11}^0$ ,  $\gamma = \frac{1}{2}$ .

Applying the previously defined algorithm to prestressed steel, it is assumed that stress  $\sigma_{ij}^0$  of values of the order 750 MPa cannot cause any change in the values of the single-crystallite elastic moduli  $c_{ij}$  of any polycrystalline aggregate (metal). On the other hand, it is supposed that changes in the values of  $L_1$ ,  $L_3$ ,  $L_5$  and  $Z$  (i.e., in the texture) are permissible if  $\sigma_{ij}^0 \leq 750$  MPa.

The numerical calculations have been performed in order to know from our own experience how the proposed algorithm is useful for acoustoelastic investigations. In this way, we have analyzed a few examples. In order to simplify the subsequent elaborations and to avoid making the paper even longer, the remainder of the paper is dealing with the numerical calculations concerning only one of the examples.

#### 4 Numerical results and discussion

In the subsequent numerical analysis, we are interested in the properties of the algorithm given by Eqs. (14)–(23), (29), (34) and in the predicted changes in the values of the ultrasonic velocities  $V_{11}, V_{22}, V_{33}, V_{12}, V_{21}, V_{13}, V_{23}, V_{31}, V_{32}$ , normalized effective elastic stiffness moduli  $\tilde{C}_{11}, \tilde{C}_{22}, \tilde{C}_{33}, \tilde{C}_{44}, \tilde{C}_{55}, \tilde{C}_{66}$ , Lagrangian multipliers  $L_1, L_3, L_5$ , and partition function  $Z$ , all the values being evaluated in the maximum-entropy approximation for a rolled steel plate subjected to plane stress with  $\tilde{\sigma}_{11}^0$  increasing from 1 MPa to 750 MPa and  $\tilde{\sigma}_{22}^0 = \frac{1}{2}\tilde{\sigma}_{11}^0$ . The other components of the plane stress  $\tilde{\sigma}_{ij}^0$  are not involved in the algorithm, after assuming  $\tilde{\sigma}_{33}^0 = 0$ . The rolled steel is assumed to be characterized by the following values of the single-crystal effective stiffness moduli and density:

$$\begin{aligned} c_{11} &= 205 \text{ GPa}, & c_{12} &= 133 \text{ GPa}, \\ c_{44} &= 125 \text{ GPa}, & \rho &= 7819 \text{ kgm}^{-3}. \end{aligned} \quad (35)$$

In examining the changes in the elastic and propagation properties of the polycrystalline aggregate as well as in the maximum-entropy probability density function,  $p(\xi, \phi)$ , the task is to determine the dependence of the Lagrangian multipliers  $L_1, L_3, L_5$ , partition function  $Z$  and the values of  $V_{11}, V_{22}, V_{33}, V_{12}, V_{21}, V_{13}, V_{23}, V_{31}, V_{32}, \tilde{C}_{11}, \tilde{C}_{22}, \tilde{C}_{33}, \tilde{C}_{44}, \tilde{C}_{55}$  and  $\tilde{C}_{66}$  on the varying (increasing) plane stresses  $\tilde{\sigma}_{11}^0$  and  $\tilde{\sigma}_{22}^0$ . These purposes are attained in tedious numerical calculations performed on the basis of the system of Eqs. (14)–(23), (29), (34). For the sake of brevity, any detailed description of the program will not be given in this paper.

In calculating the changes in the dynamical properties and texture of the polycrystalline material, the stresses  $\sigma_{11}^0$  and  $\sigma_{22}^0 = \frac{1}{2}\sigma_{11}^0$  have been assumed to be increasing from 1 MPa to 750 MPa and from 0.5 MPa to 375 MPa, respectively, in 750 equal and rather small steps  $\Delta\sigma_{11}^0 = 1$  MPa,  $\Delta\sigma_{22}^0 = 0.5$  MPa. For every 750 pairs of  $\sigma_{11}^0$  and  $\sigma_{22}^0$  values, a running program of the calculation is a succession of successful and fruitless iteration steps. If an iteration step leads to increase the calculation accuracy it is successful; otherwise, it is fruitless. In performing the calculation it is necessary to have a check of the current accuracy of the calculation. Therefore, it is necessary to evolve an error parameter  $Qm$ . In order to define this parameter, let us focus our attention again on the right-hand parts of Eqs. (14)–(19) and call them Eqs. (14<sup>r</sup>)–(19<sup>r</sup>). Now denote by  $R(l)$  and  $L(l)$ ,  $l = 14, 15, \dots, (19)$ , the values of the right- and left-hand sides of Eqs. (14<sup>r</sup>)–(19<sup>r</sup>), respectively, which are calculated after every successful iteration step. Then we can define the maximum relative error  $Qm$  of finding the current values of  $L_k$ ,  $k = 1, 3, 5, Z, V_{11}, V_{22}, V_{33}, V_{12}, V_{21}, V_{13}, V_{23}, V_{31}, V_{32}$  as follows:

$$Qm = \text{DMAX1}[Gm(14), Gm(15), \dots, Gm(19)], \quad (36)$$

where **DMAX1** is the FORTRAN intrinsic function, which returns the maximum value in the argument list. The nomenclature introduced in the last equation is as follows:

$$Gm(l) = \text{DABS}\{[R(l) - L(l)]/L(1)\}, \quad l = 14, 15, \dots, (19), \quad (37)$$

where the FORTRAN intrinsic function **DABS** returns the absolute value of its argument,

The numerical calculations, whose results are presented in the paper in Figs. 1–3, have been performed with the maximum relative error  $Qm = 5.5 \cdot 10^{-5}$ . The consequences of this error to the values of  $V_{ij}$  is, consistent with that of the error  $\pm 0.5 \text{ ms}^{-1}$  of the respective ultrasonic measurements.

Figure 1 shows the plots of  $L_1, L_3, L_5$ , and  $Z$  versus  $\tilde{\sigma}_{11}^0$ . The values of  $L_1, L_3, L_5$ , and  $Z$  vary monotonously from 3.41241, 11.3020,  $-4.07668$ , 13, 3875 for  $\sigma_{11}^0 = 1$  MPa to 3.20248, 11.5754,

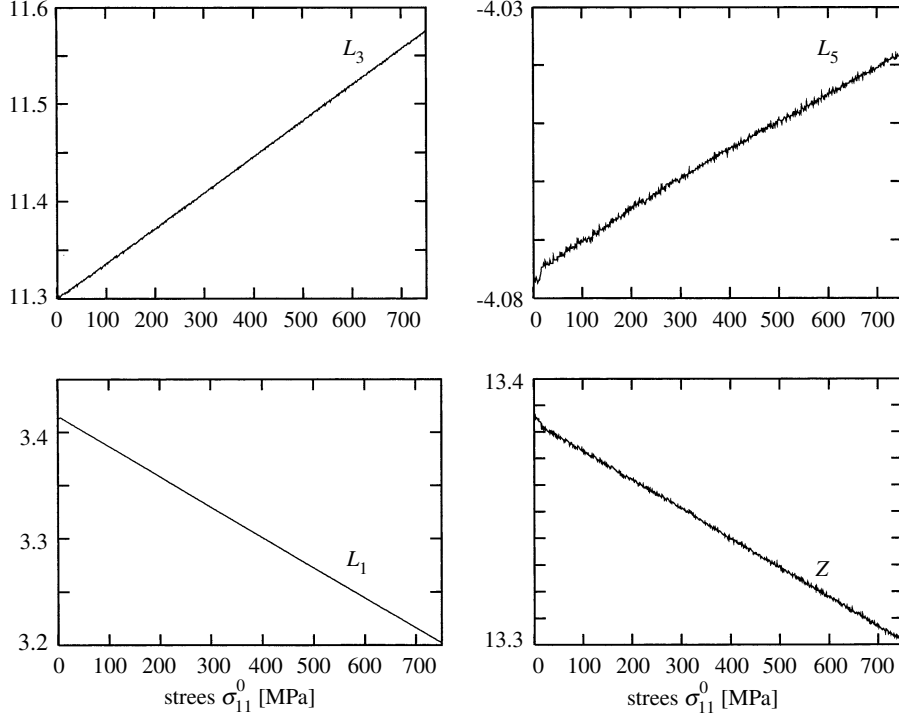


**Fig. 1.** Lagrangian multipliers  $L_1$ ,  $L_3$ ,  $L_5$  and partition function  $Z$  versus the stress  $\sigma_{11}^0$

$-4.03822$ ,  $13.3010$  for  $\sigma_{11}^0 = 750$  MPa, respectively, with increasing  $\sigma_{11}^0$  and  $\sigma_{22}^0 = \frac{1}{2}\sigma_{11}^0$ . In order to evaluate the influence of these changes in the values of  $L_1$ ,  $L_3$ ,  $L_5$ , and  $Z$  on the theoretically predicted distribution of the single-crystallite orientation, let us utilize the quantities defined by the following equations:

$$n_\varphi(\varphi_1, \varphi_2; \sigma_{11}^0 = \sigma_m) = \int_{-1}^1 d\xi \int_{\varphi_1}^{\varphi_2} d\varphi \int_0^{2\pi} d\phi p(\xi, \varphi, \phi), \quad (38)$$

$$n_\phi(\phi_1, \phi_2; \sigma_{11}^0 = \sigma_m) = \int_{-1}^1 d\xi \int_0^{2\pi} d\varphi \int_{\phi_1}^{\phi_2} d\phi p(\xi, \varphi, \phi), \quad (39)$$

$$n_\theta(\xi_1, \xi_2; \sigma_{11}^0 = \sigma_m) = \int_{\xi_2}^{\xi_1} d\xi \int_0^{2\pi} d\varphi \int_0^{2\pi} d\phi p(\xi, \varphi, \phi). \quad (40)$$

These quantities characterize the distribution of the single-crystallite orientation in the polycrystalline aggregate subjected to the plane stress  $\sigma_{ij}^0$  with  $\sigma_{11}^0 = \sigma_m$  and  $\sigma_{22}^0 = \frac{1}{2}\sigma_m$ ,  $0 \leq \sigma_m \leq 750$  MPa, namely  $n_\theta(\xi_1, \xi_2; \sigma_{11}^0 = \sigma_m)$ ,  $n_\varphi(\varphi_1, \varphi_2; \sigma_{11}^0 = \sigma_m)$  and  $n_\phi(\phi_1, \phi_2; \sigma_{11}^0 = \sigma_m)$ . denote the fractions of the total number of crystallites in the material with the angle of nutation,  $\theta$ , lying in the interval  $\theta_1 \leq \theta \leq \theta_2$  (where  $\theta_1 = \cos^{-1} \xi_1$ ,  $\theta_2 = \cos^{-1} \xi_2$ ), with the angle of precession,  $\varphi$ , lying in the interval  $\varphi_1 \leq \varphi \leq \varphi_2$  and with the angle of proper

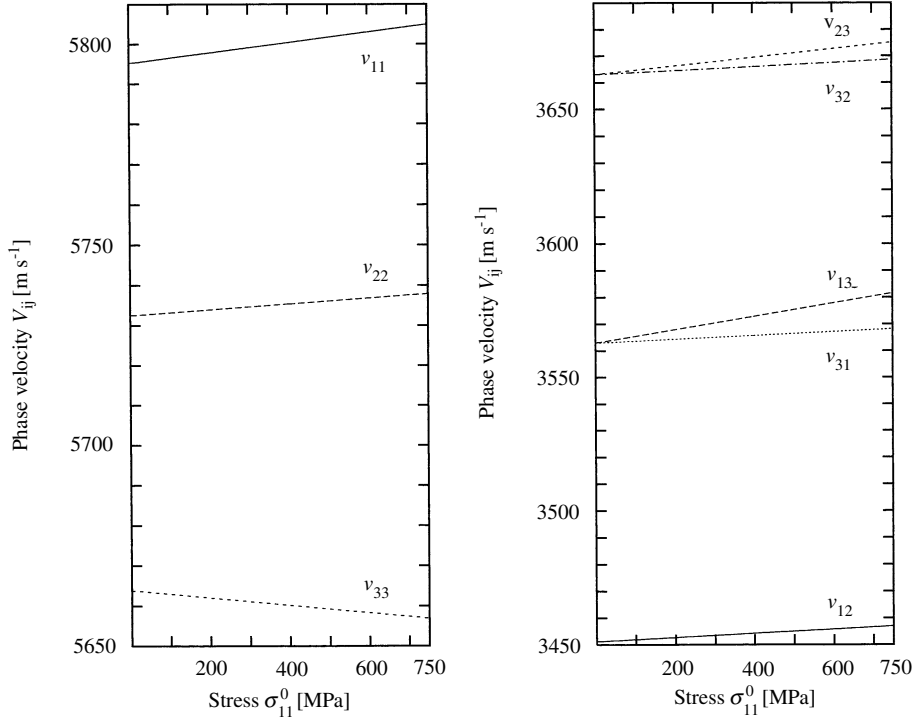


**Fig. 2.** Ultrasonics phase velocities  $V_{11}$ ,  $V_{22}$ ,  $V_{33}$ ,  $V_{12}$ ,  $V_{13}$ ,  $V_{31}$ ,  $V_{23}$ , and  $V_{32}$  versus the stress  $\sigma_{11}^0$

rotation,  $\phi$ , lying in the interval  $\phi_1 \leq \phi \leq \phi_2$ , respectively. The numerical calculations of  $n_\varphi(\varphi_1, \varphi_2; \sigma_{11}^0 = \sigma_m)$ ,  $n_\phi(\phi_1, \phi_2; \sigma_{11}^0 = \sigma_m)$  and  $n_\theta(\xi_1, \xi_2; \sigma_{11}^0 = \sigma_m)$  have been performed with the whole domains  $[0, 360]$  of the angles of precession  $\varphi$  and proper rotation  $\phi$  as well as with the whole domain  $[0, 180]$  of the angle of nutation  $\theta$ , the domains being divided into parts (subdomains) of equal size of 18 with centres at  $\varphi_c$ ,  $\phi_c$  and  $\theta_c$ , respectively. Hence,

$$\left. \begin{aligned} \varphi_c &= (\varphi_k + \varphi_{k+1})/2 \\ \phi_c &= (\phi_l + \phi_{l+1})/2 \end{aligned} \right\} = 9^\circ, 27^\circ, \dots, 351^\circ; \quad k, l = 0, 1, \dots, 19,$$

$$\left. \begin{aligned} \varphi_0, \varphi_1, \dots, \varphi_{20} \\ \phi_0, \phi_1, \dots, \phi_{20} \end{aligned} \right\} = 0^\circ, 18^\circ, \dots, 360^\circ; \quad \theta_c = (\theta_m + \theta_{m+1})/2 = 9^\circ, 27^\circ, \dots, 171^\circ;$$

$$m = 0, 1, \dots, 9; \quad \theta_0, \theta_1, \dots, \theta_{10} = 0^\circ, 18^\circ, \dots, 180^\circ.$$

Making use of Eqs. (38)–(40), we define the following quantities:

$$\Delta n_\varphi\{\xi_1, \xi_2; \sigma_{11}^0(1 \nearrow 750)\} = \frac{n_\varphi(\varphi_1, \varphi_2; \sigma_{11}^0 = 750) - n_\varphi(\varphi_1, \varphi_2; \sigma_{11}^0 = 1)}{n_\varphi(\varphi_1, \varphi_2; \sigma_{11}^0 = 1)}, \quad (41)$$

$$\Delta n_\phi\{\xi_1, \xi_2; \sigma_{11}^0(1 \nearrow 750)\} = \frac{n_\phi(\phi_1, \phi_2; \sigma_{11}^0 = 750) - n_\phi(\phi_1, \phi_2; \sigma_{11}^0 = 1)}{n_\phi(\phi_1, \phi_2; \sigma_{11}^0 = 1)}, \quad (42)$$

$$\Delta n_\theta\{\xi_1, \xi_2; \sigma_{11}^0(1 \nearrow 750)\} = \frac{n_\theta(\xi_1, \xi_2; \sigma_{11}^0 = 750) - n_\theta(\xi_1, \xi_2; \sigma_{11}^0 = 1)}{n_\theta(\xi_1, \xi_2; \sigma_{11}^0 = 1)}. \quad (43)$$

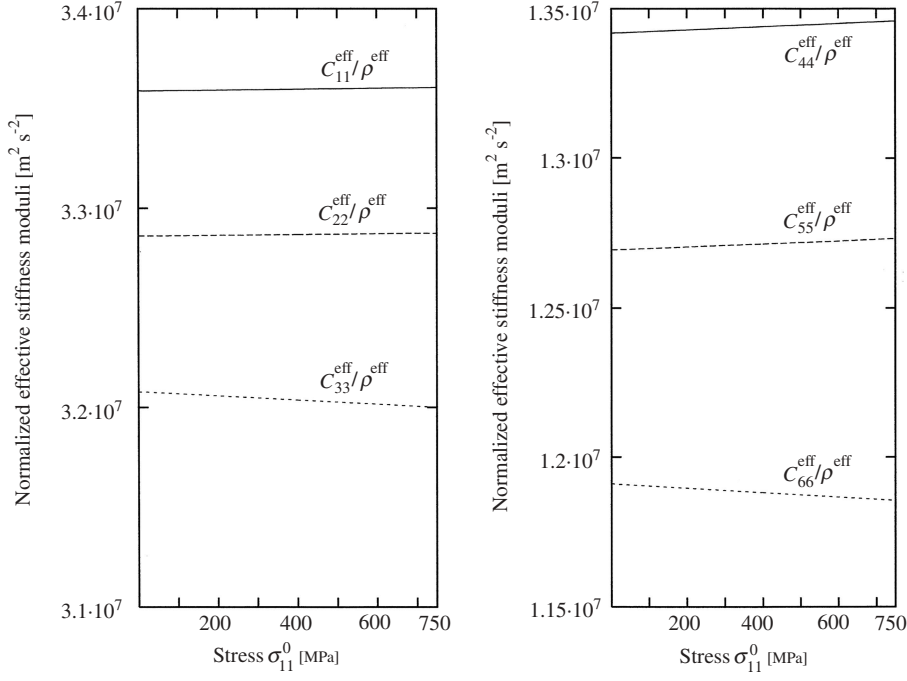


**Fig. 3.** Normalized effective stiffness moduli  $\tilde{C}_{11}^{\text{eff}}$ ,  $\tilde{C}_{22}^{\text{eff}}$ ,  $\tilde{C}_{33}^{\text{eff}}$ ,  $\tilde{C}_{44}^{\text{eff}}$ ,  $\tilde{C}_{55}^{\text{eff}}$ , and  $\tilde{C}_{66}^{\text{eff}}$  versus the stress  $\sigma_{11}^0$

The quantities  $\Delta n_\varphi\{\xi_1, \xi_2; \sigma_{11}^0(1 \nearrow 750)\}$ ,  $\Delta n_\phi\{\xi_1, \xi_2; \sigma_{11}^0(1 \nearrow 750)\}$ , and  $\Delta n_\theta\{\xi_1, \xi_2; \sigma_{11}^0(1 \nearrow 750)\}$ , which in Table 1 are denoted by  $\Delta n_\varphi$ ,  $\Delta n_\phi$ ,  $\Delta n_\theta$ , respectively, characterize the relative changes in the distribution of the single-crystallite orientation in the polycrystalline aggregate subjected to the plane background stress ( $\sigma_{11}^0 \neq 0$ ,  $\sigma_{22}^0 \neq 0$ ,  $\sigma_{33}^0 = 0$ ), the changes being induced by the stress increase from  $\sigma_{11}^0 = 1\text{MPa}$  to  $\sigma_{11}^0 = 750\text{MPa}$  with  $\sigma_{22}^0 = \frac{1}{2}\sigma_{11}^0$  and  $\sigma_{33}^0 = 0$ . The predicted values of the quantities  $n_\varphi(\varphi_1, \varphi_2; \sigma_{11}^0 = 1)$ ,  $n_\phi(\phi_1, \phi_2; \sigma_{11}^0 = 1)$ ,  $n_\theta(\xi_1, \xi_2; \sigma_{11}^0 = 1)$ ,  $\Delta n_\varphi\{\xi_1, \xi_2; \sigma_{11}^0(1 \nearrow 750)\}$ ,  $\Delta n_\phi\{\xi_1, \xi_2; \sigma_{11}^0(1 \nearrow 750)\}$ ,  $\Delta n_\theta\{\xi_1, \xi_2; \sigma_{11}^0(1 \nearrow 750)\}$  calculated from Eqs. (36)–(41), respectively, are given in Table 1. In the first column of Table 1, the angle intervals  $0^\circ - 18^\circ$ ,  $18^\circ - 36^\circ$ ,  $\dots$ ,  $162^\circ - 180^\circ$  correspond to the intervals  $\Delta\varphi$ ,  $\Delta\phi$ ,  $\Delta\theta$  of the angles  $\varphi$ ,  $\phi$  and  $\theta$ , respectively. The bottom horizontal line of Table 1, which corresponds to the values  $\varphi, \phi, \theta = 180^\circ$ , would be the axis of the mirror symmetry of the parts (columns  $n_\varphi, \Delta n_\varphi, n_\phi, \Delta n_\phi$ ) of Table 1 if they were lengthened to concern the angles  $0^\circ \leq \varphi \leq 360^\circ$  and  $0^\circ \leq \phi \leq 360^\circ$ . This fact is a consequence of the orthorhombic symmetry of the polycrystalline aggregate under consideration. For this reason, in Table 1 there are given only the halves of the columns  $n_\varphi, \Delta n_\varphi, n_\phi$ , and  $\Delta n_\phi$  which correspond to  $0^\circ \leq \varphi \leq 180^\circ$  and  $0^\circ \leq \phi \leq 180^\circ$ .

The results of the numerical calculations given in Table 1 in the columns entitled  $\Delta n_\varphi$ ,  $\Delta n_\phi$  and  $\Delta n_\theta$  reveal that the presented considerations predict small influence of the plane stress  $\sigma_{ij}^0$  on the texture. This small effect of the stress  $\sigma_{ij}^0$  on the texture ( $p(\theta, \varphi, \phi)$ ) is also revealed in Fig. 1 by small changes in the values of the Lagrangian multipliers  $L_1, L_3, L_5$  and partition function  $Z$  with the varying (increasing) plane stress  $\sigma_{ij}^0$ . It can easily be seen from Figs. 2 and 3 that, contrary to the texture, some acoustoelastic properties of the polycrystalline aggregate subjected to the varying stress  $\sigma_{ij}^0$  are significantly affected by the stress.

**Table 1.** Texture estimation of the prestressed polycrystalline aggregate

$\Delta\varphi \Delta\phi \Delta\theta$	$n_\varphi$ and $\Delta n_\varphi$		$n_\phi$ and $\Delta n_\phi$		$n_\theta$ and $\Delta n_\theta$	
	$n_\varphi$ Eq. (38)	$\Delta n_\varphi$ Eq. (41)	$n_\phi$ Eq. (39)	$\Delta n_\phi$ Eq. (42)	$n_\theta$ Eq. (40)	$\Delta n_\theta$ Eq. (43)
0°–18°	$7.26 \cdot 10^{-2}$	$7.15 \cdot 10^{-3}$	$6.27 \cdot 10^{-2}$	$-7.54 \cdot 10^{-3}$	$6.86 \cdot 10^{-2}$	$1.88 \cdot 10^{-2}$
18°–36°	$3.84 \cdot 10^{-2}$	$-8.54 \cdot 10^{-3}$	$4.77 \cdot 10^{-2}$	$5.66 \cdot 10^{-3}$	$6.99 \cdot 10^{-2}$	$-6.51 \cdot 10^{-3}$
36°–54°	$2.79 \cdot 10^{-2}$	$-1.37 \cdot 10^{-2}$	$3.91 \cdot 10^{-2}$	$1.33 \cdot 10^{-2}$	$4.52 \cdot 10^{-2}$	$-2.88 \cdot 10^{-2}$
54°–72°	$3.84 \cdot 10^{-2}$	$-8.56 \cdot 10^{-3}$	$4.38 \cdot 10^{-2}$	$5.31 \cdot 10^{-3}$	$8.59 \cdot 10^{-2}$	$-1.59 \cdot 10^{-2}$
72°–90°	$7.26 \cdot 10^{-2}$	$7.16 \cdot 10^{-3}$	$5.66 \cdot 10^{-2}$	$-9.70 \cdot 10^{-3}$	$2.30 \cdot 10^{-1}$	$7.93 \cdot 10^{-3}$
90°–108°	$7.26 \cdot 10^{-2}$	$7.16 \cdot 10^{-3}$	$5.66 \cdot 10^{-2}$	$-9.70 \cdot 10^{-3}$	$2.30 \cdot 10^{-1}$	$7.93 \cdot 10^{-3}$
108°–126°	$3.84 \cdot 10^{-2}$	$-8.56 \cdot 10^{-3}$	$4.38 \cdot 10^{-2}$	$5.31 \cdot 10^{-3}$	$8.59 \cdot 10^{-2}$	$-1.59 \cdot 10^{-2}$
126°–144°	$2.79 \cdot 10^{-2}$	$-1.37 \cdot 10^{-2}$	$3.91 \cdot 10^{-2}$	$1.33 \cdot 10^{-2}$	$4.51 \cdot 10^{-2}$	$-2.89 \cdot 10^{-2}$
144°–162°	$3.84 \cdot 10^{-2}$	$-8.56 \cdot 10^{-3}$	$4.77 \cdot 10^{-2}$	$5.67 \cdot 10^{-3}$	$6.98 \cdot 10^{-2}$	$-6.57 \cdot 10^{-3}$
162°–180°	$7.26 \cdot 10^{-2}$	$7.16 \cdot 10^{-3}$	$6.27 \cdot 10^{-2}$	$-7.55 \cdot 10^{-3}$	$6.88 \cdot 10^{-2}$	$1.89 \cdot 10^{-2}$

Certainly, the theoretical predictions of the algorithm are influenced on by the simplifying assumptions of the considerations presented in the paper, which have led us to the algorithm. The fitness of the predictions of the algorithm with experimental results would be revealed if the experiments were performed. Now we confine ourselves only to try to perceive some tendencies of the algorithm in its predicting of the changes in acoustoelastic properties of the polycrystalline aggregate in the situation when the changes in the texture increase slowly with the increasing background stress.

Suppose that the values of  $L_1, L_3, L_5, Z, V_{11}, V_{22}, V_{33}, V_{12}, V_{21}, V_{13}, V_{23}, V_{31}, V_{32}, \tilde{C}_{11}, \tilde{C}_{22}, \tilde{C}_{33}, \tilde{C}_{44}, \tilde{C}_{55},$  and  $\tilde{C}_{66}$  have been found for the orthorhombic polycrystalline aggregate which was assumed to be approximately free of stress ( $\sigma_{11}^0 = 1 \text{ MPa} \approx 0, \sigma_{22}^0 = 0.5 \text{ MPa} \approx 0, \sigma_{33}^0 = 0$ ) at the start of computing. Figures 1–3 and Tables 1 and 2 show some predictions of the algorithm in the situation when the background stresses  $\sigma_{11}^0 \neq 0, \sigma_{22}^0 \neq 0$  and  $\sigma_{33}^0 = 0$  increase from  $\sigma_{11}^0 = 1 \text{ MPa}$  to  $\sigma_{11}^0 = 750 \text{ MPa}$  with  $\sigma_{33}^0 = 0$  and  $\sigma_{22}^0 = \frac{1}{2}\sigma_{11}^0$  in 750 equal steps, and simultaneously  $C_{11}, C_{12}, C_{44}$  retain their constant values.

Now let us give some comments on the results of the numerical analysis, the considered results being presented in Figs. 1–3 and Tables 1 and 2.

- (i) It should perhaps be stressed at first that the presented predictions have been obtained by using the algorithm deduced under the assumption that the single-crystal effective stiffness moduli  $c_{11}, c_{12}$  and  $c_{44}$  retain their constant values with increasing background stresses  $\sigma_{ii}^0, ii = 11, 22, 33$ . This assumption is not in contradiction to another assumption that the background stresses  $\sigma_{ii}^0$  are increasing only up to the values at which there still does not occur any significant effect of plastic deformation on the texture (i.e, on the shape of  $p(\theta, \varphi, \phi)$ ), the texture being determined by the Lagrangian multipliers  $L_1, L_3, L_5$  and the partition function  $Z$ . These assumptions
- allow us to use for all considered values of the background stresses the same algorithm in computing the values of the quantities being of interest for us;
  - in discussing the obtained numerical results, allow us both to regard the Lagrangian multipliers and partition function as functions of the background stresses  $\sigma_{ii}^0, ii = 11, 22, 33$  and to suppose that good approximations of these functions may be of the form of the power series with respect to the background stresses  $\sigma_{ii}^0$ , each of the series being truncated after the terms linear in  $\sigma_{ii}^0$ . In the computations presented here,  $\sigma_{22}^0 = \gamma \cdot \sigma_{11}^0, \gamma = 0.5, \sigma_{33}^0 = 0$ . Hence there are approximately linear dependences of the numerically computed values of the quantities  $L_1, L_3, L_5$  and  $Z$  on the stress  $\sigma_{11}^0$ .

**Table 2.** Computed changes in the values of some quantities  $F$  in the prestressed polycrystalline aggregate

$F$	$F_1 \doteq F(\sigma_{11}^0 = 1 \text{ Mpa})$	$F_{750} \doteq F(\sigma_{11}^0 = 750 \text{ Mpa})$	$\Delta F \doteq (F_{750} - F_1)/F_1$
$L_1$	3.412417698197	3.202480799663	-0.061521
$L_3$	11.30196649049	11.57547247279	0.024200
$L_5$	-4.076682080805	-4.038222859390	0.0094340
$Z$	13.3875	13.3010	-0.0064613
$\tilde{C}_{11}^{eff}$ [ $\text{m}^2\text{s}^{-2}$ ]	$3.35855 \cdot 10^7$	$3.36017 \cdot 10^7$	0.00048235
$\tilde{C}_{22}^{eff}$ [ $\text{m}^2\text{s}^{-2}$ ]	$3.28625 \cdot 10^7$	$3.28757 \cdot 10^7$	0.00040167
$\tilde{C}_{33}^{eff}$ [ $\text{m}^2\text{s}^{-2}$ ]	$3.20784 \cdot 10^7$	$3.20009 \cdot 10^7$	-0.0024160
$\tilde{C}_{44}^{eff}$ [ $\text{m}^2\text{s}^{-2}$ ]	$3.34181 \cdot 10^7$	$1.34587 \cdot 10^7$	0.0030258
$\tilde{C}_{55}^{eff}$ [ $\text{m}^2\text{s}^{-2}$ ]	$1.26951 \cdot 10^7$	$1.27320 \cdot 10^7$	0.0029066
$\tilde{C}_{66}^{eff}$ [ $\text{m}^2\text{s}^{-2}$ ]	$1.19110 \cdot 10^7$	$1.18549 \cdot 10^7$	-0.0047099
$V_{31}^2$ [ $\text{m}^2\text{s}^{-2}$ ]	12695111	12731980	0.0022904
$V_{32}^2$ [ $\text{m}^2\text{s}^{-2}$ ]	13418082	13458699	0.0030270
$V_{33}^2$ [ $\text{m}^2\text{s}^{-2}$ ]	32078403	32000970	-0.0024139
$V_{11}^2$ [ $\text{m}^2\text{s}^{-2}$ ]	33585618	33697677	0.0033365
$V_{12}^2$ [ $\text{m}^2\text{s}^{-2}$ ]	11911126	11950780	0.0033291
$V_{22}^2$ [ $\text{m}^2\text{s}^{-2}$ ]	32862588	32923726	0.0018604
$V_{13}^2$ [ $\text{m}^2\text{s}^{-2}$ ]	12695254	12827858	0.0104452
$V_{23}^2$ [ $\text{m}^2\text{s}^{-2}$ ]	13418155	13506654	0.0065955

In this way, we arrive at the conclusions that the changes in the values of the statistical moments  $\langle r_t(\xi, \varphi, \phi) \rangle$ ,  $t = 1, 2, \dots, 6$ , with increasing background stresses  $\sigma_{ii}^0$  may be expected to be also small. Consequently, the right-hand parts of Eqs. (14)–(19) imply that the stress-induced changes  $\Delta\tilde{C}(\sigma_{ii}^0)_u$  can be written in a good approximation also in the form of the power series with respect to  $\sigma_{ii}^0$ , the series being reduced (truncated) to the sum of the terms of zeroth- and linear-order in  $\sigma_{ii}^0$ . In this way, for the case of  $\sigma_{22}^0 = \gamma$ ,  $\sigma_{11}^0, \gamma = 0.5$ ,  $\sigma_{33}^0 = 0$  and for each propagation velocity  $V_{ij}$ ,  $i, j = 1, 2, 3$ , we can obtain, from the right-hand part of the respective one of Eqs. (14)–(19), relationships like the following ones for  $V_{11}$  from the right-hand part of Eqs. (14):

$$\begin{aligned}
V(\tilde{\sigma}_{11}^0)_{11} &= [\tilde{C}(\tilde{\sigma}_{11}^0)_{11} + \tilde{\sigma}_{11}^0]^{1/2} \Leftrightarrow V(\tilde{\sigma}_{11}^0)_{11} = [\tilde{C}(\tilde{\sigma}_{11}^0 = 0)_{11} + \Delta\tilde{C}(\tilde{\sigma}_{11}^0)_{11} + \tilde{\sigma}_{11}^0]^{1/2} \\
&\cong [\tilde{C}(\tilde{\sigma}_{11}^0 = 0)_{11}]^{1/2} \cdot \left\{ 1 + \frac{1}{2} [\Delta\tilde{C}(\tilde{\sigma}_{11}^0)_{11} / \tilde{C}(\tilde{\sigma}_{11}^0 = 0)_{11} + \tilde{\sigma}_{11}^0 / \tilde{C}(\tilde{\sigma}_{11}^0 = 0)_{11}] \right\}. \quad (44)
\end{aligned}$$

Hence there is an approximately linear dependence of the computed values of each propagation velocity  $V_{ij}$ ,  $i, j = 1, 2, 3$ , on the stress  $\sigma_{11}^0$ .

- (ii) Let us remind that in the numerical analysis in the present paper we are interested in the situation where the initially stress-free (or approximately stress-free) bulk sample of the textured polycrystal is subjected to small applied stresses  $\Delta\sigma_{ij}^0 \leq 1 \text{ MPa}$ ,  $i, j = 1, 2, 3$ . After approaching the equilibrium deformed configuration of the material points of the body, the values of the applied stresses are increased again by the same constant and small steps  $\Delta\sigma_{ij}^0$ , and, consequently, the material points of the bulk sample tend to a new equilibrium deformed configuration. The sequences of two following events: increasing the applied stresses  $\sigma_{ij}^0$  by the successive steps  $\Delta\sigma_{ij}^0$  and then approaching the new equilibrium deformed

configuration of the body material points are repeated as many times ( $N = 750$ ) as the applied stresses  $\sigma_{ij}^0 = n \cdot \Delta\sigma_{ij}^0$ ,  $n = 1, 2, \dots, N$  reach the desired limiting values  $N \cdot \Delta\sigma_{ij}^0$ . Simultaneously, the plane wave motion governed by Eqs. (8) is superimposed successively on each of the equilibrium deformed configurations of the body materials points. Strictly speaking, we substitute into Eqs. (8) its plane wave solution  $\langle \mathbf{u}(\mathbf{x}, \mathbf{t}) \rangle$  which is given by Eqs. (9)–(11), successively in the form of each of the nine wave modes (11), the phase velocities  $V_{ij}$ ,  $i, j = 1, 2, 3$ , normalized effective moduli,  $\tilde{C}_{ijkl} = C_{ijkl}^{eff} / \rho$ ,  $i, j, k, l = 1, 2, 3$  and Eqs. (8) being referred to the currently considered equilibrium deformed configuration of the material points of the body. There are numerous procedures of approximating the  $C_{ijkl}^{eff}$  proposed by such authors as Voigt [8], Reuss [16] and Hill [17]. In the present paper, we confine ourselves to considering only the case when  $C_{ijkl}^{eff}$ ,  $i, j, k, l = 1, 2, 3$ , are calculated using the Voigt averaging procedure. We do that for the following reasons:

- (a) Allen et al. [18] used neutron diffraction to measure the texture (distribution function of the crystallite orientation) of a bulk sample of highly textured and stress-free austenitic weld material. The values of the ultrasonic velocities  $V_{ij}$  in three orthogonal directions in the sample were calculated from the measured texture by using successively the Voigt, Reuss and Hill approximations (averaging procedures), and next the calculated values were compared with the measured ones of the same ultrasonic velocities  $V_{ij}$ . The Voigt approximation is found to give good agreement with experiment and appears to be the most useful approach for the calculation of ultrasonic velocities in highly textured materials [18, p. 555].
- (b) Inverting successively the averaging procedures of Voigt, Reuss and Hill, Lewandowski [5] determined three maximum-entropy estimates of the function  $p(\theta, \varphi, \phi)$  for the orthorhombically textured and stress-free polycrystalline aggregate. Each of the three estimates was determined from the same three ultrasonic velocities  $v_{ij}$ , which were regarded as known (observables) and chosen from the set of nine velocities  $v_{ij}$ ,  $i, j = 1, 2, 3$ , in such a way that each of the numbers 1, 2 and 3 appeared as subscripts  $i$  or  $j$  at no more than two velocities  $v_{ij}$ . It can readily be verified [5, p. 233] that the knowledge (measurement) of the values of three such velocities is sufficient for the set of nine values of the velocities  $v_{ij}$ ,  $i, j = 1, 2, 3$ , to be determined from the symmetry conditions (orthorhombic for the bulk sample and cubic for the grains). Next the values of another ultrasonic velocities  $V_{ij}$  were calculated in four ways: Firstly, in three ways by employing successively each of the three averaging procedures together with the estimate of the function  $p(\theta, \varphi, \phi)$  implied, in the previous step, by inverting the same averaging procedure. Secondly, in one way immediately from three known velocities  $V_{ij}$  (observables) and the symmetry conditions. Afterwards, the results of calculating the values of the same ultrasonic velocities  $V_{ij}$  from the symmetry conditions and by employing successively one of three estimates of  $p(\theta, \varphi, \phi)$  together with the averaging procedure, which had yielded the  $p(\theta, \varphi, \phi)$  in the previous step, were successively compared with each other in pairs, for each of the three applied averaging procedures, to verify the usefulness of each of the proposed methods of estimating the texture (i.e., of finding the function  $p(\theta, \varphi, \phi)$ ) from the measurements of the respective three ultrasonic velocities  $V_{ij}$ . In these tests, the velocities  $V_{ij}$  in every pair with one velocity value deduced from  $p(\theta, \varphi, \phi)$  by employing the Voigt averaging procedure, fitted approximately the same values with the best accuracy as compared with  $V_{ij}$  in each other pairs with one velocity value deduced from the Reuss and Hill averaging procedure. Therefore, it was concluded

that inverting the Voigt averaging procedure leads to such a maximum-entropy estimate of the probability density function of the crystallite orientation,  $p(\theta, \varphi, \phi)$ , that the medium acoustic anisotropy implied by this function approximates with the best accuracy the acoustic anisotropy deduced from the three observed velocities  $V_{ij}$  and symmetry rules. The results suggest that the Voigt averaging procedure is the most suitable one (as compared with that of Reuss and Hill) for estimating the effective acoustoelastic properties of the polycrystalline aggregate from its maximum-entropy estimate of the texture.

Generally, the results of numerical experiments suggest that the smaller the plane stresses  $\sigma_{11}^0$  and  $\sigma_{22}^0$  at the start of computing as well as the smaller the stress steps  $\Delta\sigma_{11}^0$  and  $\Delta\sigma_{22}^0$ , the better the agreement in the values of the theoretically predicted texture and ultrasonic velocities  $V_{11}$ ,  $V_{22}$ ,  $V_{33}$ ,  $V_{12}$ ,  $V_{21}$ ,  $V_{13}$ ,  $V_{23}$ ,  $V_{31}$ ,  $V_{32}$  with that obtained experimentally, if the respective experiments were performed. Such ultrasonic experiments would also be the most infallible method of determining the stress upper limit of applicability of the algorithm for a given set of the values of the algorithm and program parameters. Moreover, if the computer analysis was accompanied by even fragmentary experimental measurements then among others (i) one would be enabled to verify the choice of the parameters and their values controlling the exactness and rate of the iteration procedures of the program, and (ii) one would be enabled to vary (respectively improve) the values of all or of some of the parameters in such a way that these changes together with other changes in the algorithm and programs would extend the applicability range of the algorithm as well as increase the rate and exactness to be consistent with that of the measurements.

## 5 Conclusions

The method proposed in this paper yields a system of integral equations for the evaluation of changes in the acoustoelastic properties and texture of the orthorhombic polycrystalline aggregate of general loading histories, including plastic deformation. The changes are assumed to be caused by varying (e.g., increasing) background stress subjected to the polycrystal body, the single-crystallite elastic moduli retaining their constant values. The principal directions of the stress are assumed to be coincident with the axes of the orthorhombic symmetry of the bulk sample. The obtained algorithm suggests, among others, performing the numerical evaluation of these changes under the assumptions that the background stress is plane and the single-crystallite elastic moduli retain their constant values. The brief summary of the main results of such an analysis and computing is:

- (i) The predicted changes in the acoustoelastic (propagation) properties of the orthorhombic polycrystalline aggregate depend on the orientation of the direction of the elastic wave propagation and polarization with respect to the principal directions of the background stress and with respect to the symmetry axis of the polycrystal as well as depend on the values of the background stresses.
- (ii) For the plane background stress not greater than 750 MPa, the absolute values of the predicted relative changes in the distribution of the single-crystallite orientation in the polycrystalline aggregate,  $\Delta n_\varphi$ ,  $\Delta n_\phi$ ,  $\Delta n_\theta$  in Table 1, are smaller than  $3.0 \cdot 10^{-2}$ .

## References

- [1] Johnson, G. C.: Acoustoelastic response of polycrystalline aggregates exhibiting transverse isotropy. *J. Nondestructive Eval.* **3**, 1–8 (1982).
- [2] Johnson, G. C.: Acoustoelastic response of a polycrystalline aggregate with orthotropic texture. *J. Appl. Mech.* **52**, 659–663 (1983).
- [3] Johnson, G. C.: The effect of texture on acoustoelasticity. Review of progress in quantitative nondestructive evaluation vol. 28 (Thomson, D. O., Chimenti, D. E., eds.), pp. 1295–1308. Plenum Press 1983.
- [4] Kroner, E.: Statistical continuum mechanics. Lecture notes. Berlin: Springer 1971.
- [5] Lewandowski, J.: Maximum-entropy estimate of the orthorhombic texture from ultrasonic measurements. *Ultrasonics* **33**, 229–238 (1995).
- [6] Lewandowski, J.: Determination of material parameters and texture of a polycrystalline aggregate from ultrasonic measurements. *NDT&E International* **32**, 383–396 (1999).
- [7] Lewandowski, J.: Evaluation of material parameters, texture and stress of a prestressed polycrystalline aggregate from ultrasonic measurements. *Arch. Acoust.* **26**, 305–329 (2001).
- [8] Voigt W.: *Lehrbuch der Krystall Physik*. Leipzig: Teubner 1928.
- [9] Jaynes, E. T.: Information theory and statistical mechanics. *Phys. Rev.* **106**, 620–630 (1957).
- [10] Man, C. S., Lu, W. Y.: Towards an acoustoelastic theory for measurement of residual stress. *J. Elasticity* **17**, 159–182 (1987).
- [11] Pao, Y. H., Sachse, W., Fukuoka, H.: Acoustoelasticity and ultrasonic measurements of residual stresses. In: *Physical acoustics* (Mason, W. P., Thurston, R. N., eds.), pp. 62–140. New York: Academic Press 1984.
- [12] Thomson, R. B., Lee, S. S., Smith, J. F.: Angular dependence of ultrasonic wave propagation in a stressed, orthorhombic continuum: theory and application to the measurement of stress and texture. *J. Appl. Phys.* **78**, 1547–1556 (1995).
- [13] Degtyar, A. D., Rokhlin, S. I.: Absolute stress determination in orthotropic materials from angular dependence of ultrasonic velocities. *J. Appl. Phys.* **78**, 1547–1556 (1995).
- [14] Sayers, C. M.: Ultrasonic velocities in anisotropic polycrystalline aggregates. *J. Phys. C.* **15**, 2157–2167 (1982).
- [15] Press, W. H., Teukolsky, S. A., Vetterling, W. T., Flannery, P. F.: *Numerical recipes in Fortran 77*, 2nd ed. The art of scientific computing. Cambridge: Cambridge University Press 1997.
- [16] Reuss, R.: Berechnung der Fließgrenze von Mischkristallen auf Grund der Plastizitätsbedingung für Einkristalle. *Z. Angew. Math. Mech.* **9**, 49–58 (1929).
- [17] Hill, R.: The elastic behaviour of a crystalline aggregate. *Proc. Phys. Soc. London A* **65**, 349–354 (1952).
- [18] Allen, A. J., Hutchings, M. T., Sayers, C. M., Allen, D. R., Smith, R. I.: Use of neutron diffraction texture measurements to establish a model for calculation of ultrasonic velocities in highly oriented austenitic weld material. *J. Appl. Phys.* **54**, 555–560 (1983).

**Author's address:** J. Lewandowski, Institute of Fundamental Technological Research, Polish Academy of Sciences, ul. Świerkowska 21 00-043 Warsaw, Poland (E-mail: jlewando5@hotmail.com)